

# Design of optimal illumination patterns in single-pixel imaging using image dictionaries

SHUMING JIAO

*Tsinghua Berkeley Shenzhen Institute (TBSI), Shenzhen, 518000, China*  
albertjiaoee@126.com

Abstract:

Single-pixel imaging (SPI) has a major drawback that the huge number of sequential illuminations for capturing one single image requires long acquisition time and high cost. Basis illumination patterns such as sinusoidal patterns in Fourier transform and Hadamard patterns are employed to enhance the imaging efficiency. The basis illumination patterns can achieve much better efficiency than random intensity illumination patterns but the performance is still sub-optimal since the basis patterns are fixed and non-adaptive for varying object images. In this work, we propose a novel scheme to design the illumination patterns adaptively when SPI is applied in a specific and pre-known imaging scenario. Exemplar training images belonging to the target specific category of object images are collected and an image dictionary is constructed in advance. Then the optimized illumination patterns are designed by extracting the common image features from the image dictionary using principal component analysis. Simulation results reveal that our proposed scheme outperforms conventional Fourier single-pixel imaging in terms of imaging efficiency.

## 1. INTRODUCTION

Single-pixel imaging (SPI) [1-3] is a novel computational imaging technique by recording an object scene using a single-pixel detector without spatial resolution. In conventional imaging, a two-dimensional object image is recorded at once by a pixelated image sensor array. In single-pixel imaging, varying illumination patterns are projected onto the object scene sequentially and a one-dimensional single-pixel intensity sequence is recorded after a large number of illuminations. Then the two-dimensional object image is computationally reconstructed from both the recorded intensity sequence and illumination patterns.

Single-pixel imaging can exhibit substantial advantages over conventional imaging under some circumstances, e. g. when the cost of pixelated image sensor is high for certain spectral bands, when no direct line of sight is available for the object scene or when the light condition is very weak. In previous works, single-pixel imaging is extensively investigated for various applications such as such as terahertz imaging [4], remote sensing [5], three-dimensional (3-D) imaging [6-8], microscopy [9, 10], scattering imaging [11], hyperspectral imaging [12], X-ray imaging [13], optical security [14,15], lidar detection [16, 17] and gas leak monitoring [18]..

Some challenges remain to be addressed for single-pixel imaging systems. One inherent drawback of single-pixel imaging system is low imaging efficiency and long image acquisition time. A reconstructed object image with reasonable quality can only be obtained when an adequate number of illuminations are sequentially projected. It will be favorable if a high-quality object image can be reconstructed using only a small number of illuminations. In previous works, the imaging efficiency of single-pixel imaging is mostly improved from two aspects: optimized reconstruction algorithms and optimized illumination patterns. In classical single-pixel imaging, often referred to as computational ghost imaging, the illumination patterns are usually random intensity patterns and the classical reconstruction algorithm is correlation method [2]. Some attempts have been made to improve the reconstruction algorithm and reduce the sampling ratio in single-pixel imaging based on random intensity illumination patterns, including differential correlation [19], normalized correlation [20], compressive sensing [21, 22], Gerchberg-

Saxton iteration [23], image sparse representation [24], measurement matrix pseudo inversion and decomposition [25, 26], deep learning [27-30]. On the other hand, the imaging efficiency is improved by designing proper basis illumination patterns such as Fourier transform sinusoidal patterns [31], Hadamard transform patterns [32], cosine transform patterns [33], and wavelet transform [34-36], instead of random intensity patterns. In a single-pixel imaging system using basis patterns, the spectrum of object image in the transformed domain can be directly acquired pixel-by-pixel with the single-pixel detector. Then the object image can be computationally reconstructed by an inverse transform. For a natural smooth image, the spectrum energy is usually concentrated in the low frequency components in the transformed domain (e.g. Fourier transform, Hadamard transform, cosine transform etc.). The object image can be approximately reconstructed from these low frequency components only and the high frequency components can be discarded. In this way, a single-pixel imaging can be realized with a significantly reduced number of illuminations.

Despite the success achieved by the abovementioned schemes, a further enhanced imaging efficiency in single-pixel imaging systems is still very favorable. In many cases, a single-pixel imaging system is usually applied to a specific scenario (such as microscopy, remote sensing and X-ray imaging), the target object images will belong to a specific image category and have some common features. The basis patterns in previous schemes [31-36] are fixed for varying categories of target object images and hence the imaging efficiency is still sub-optimal. In this paper, optimized illumination patterns are designed for each different category of object images adaptively by extracting the common image features from pre-given image dictionaries using principal component analysis (PCA) algorithm. It shall be noticed that, the concept of image dictionary and the concept of principal component analysis (singular value decomposition) are attempted in previous single-pixel imaging works [24, 26]. But these works [24, 26] focuses on the optimal reconstruction algorithms when the illumination patterns are random intensity patterns

in SPI. The objective of this work to design optimal illumination patterns using image dictionaries and principal component analysis (singular value decomposition) algorithm in SPI.

## 2. PROPOSED ILLUMINATION PATTERN DESIGN SCHEME FOR SINGLE-PIXEL IMAGING SCHEME

The optical setup for a single-pixel imaging system is shown in Figure 1.

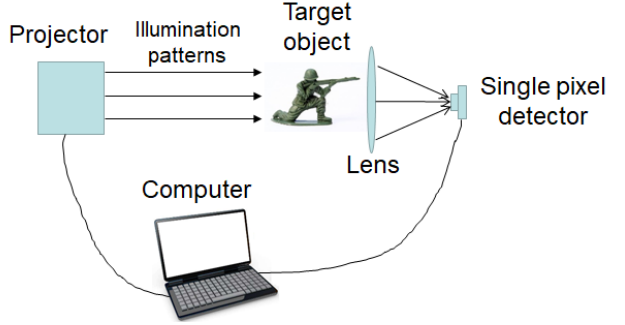


Fig. 1. Optical setup for a single-pixel imaging system.

In single-pixel imaging, varying illumination patterns are projected from a spatial light modulator (SLM) or Digital Mirror Device (DMD) device onto the object image sequentially. Then the total light intensity, mathematically the inner product between the object image and the illumination patterns, is recorded by a single-pixel detector. Finally, the object image is computationally reconstructed from the illumination patterns and single-pixel intensity sequence recorded.

It is assumed that the spatial resolution of each illumination pattern, or the total number of pixels in the pattern, is  $N = X \times Y$ . In fact, this resolution is identical to the object image resolution in the imaging model. In our proposed scheme, a number of exemplar object images (training images) need to be collected in advance to constitute an image dictionary for a specific imaging scenario. Then the optimal illumination patterns are designed based on the common features extracted from the image dictionaries and can be applied to any target object image similar to the exemplar images in the dictionary. It is assumed that totally  $M$  training images are used in the dictionary and each image is represented by a row vector of length  $N$ . A two-dimensional matrix  $A$  with size  $M \times N$  can be employed to represent all the training images. A principal component analysis (PCA) [37-42], or singular vector decomposition, can be performed on

the matrix  $A$  to decompose the matrix into eigenvalues and eigenvectors. According to the mechanism of PCA, the training image matrix  $A$  can be expressed in the following form shown in Eqs. (1)

$$A = P\Delta Q = WQ \quad (1)$$

where  $P$  is the eigenvector matrix of  $AA^T$  ( $A^T$  is the transposed matrix of  $A$ ) with size  $M \times K$  (each column is an eigenvector),  $Q$  is the eigenvector matrix of  $A^T A$  with size  $K \times N$  (each row is an eigenvector) and  $\Delta$  is a diagonal matrix containing the  $K$  largest eigenvalues for  $AA^T$  and  $A^T A$  ( $1 \leq K \leq N$ ). Alternatively,  $A$  can be represented as a multiplication of weighting coefficient matrix  $W$  (size  $M \times K$ ) and basis pattern matrix  $Q$ .

From a statistical point of view, PCA is a transform that converts a set of observations of  $M$  correlated variables into a weighted combination of  $K$  orthogonal uncorrelated basis variables (principal components). Here in our case, each variable is equivalent to an object image and each observation is equivalent to a pixel intensity in the image. PCA can perform data reduction since the  $K$  principal components can account for most of the variability in the original  $M$  variables. In previous works, PCA has been extensively employed in data compression and dimension reduction applications [37-42].

One arbitrary row vector  $a$  (size  $1 \times N$ ) in the matrix  $A$ , representing one single training object image, can be expressed as Eqs. (2)

$$a = \sum_{k=1}^K w_k q_k \quad (2)$$

where  $q_k$  is the  $k$ th row of matrix  $Q$ , representing the  $k$ th basis pattern (or  $k$ th principal component) and  $w_k$  denotes the  $k$ th weighting coefficient for the corresponding principal component for the object image  $a$ . The  $K$  principal components are orthogonal between each other, similar to the basis patterns in Fourier transform, Hadamard transform or other transforms, shown in Eqs. (3).

$$\sum_{s=1}^N q_{is} q_{js} = 1 \quad (i = j) \text{ or } 0 \quad (i \neq j) \quad (3)$$

where  $q_{is}$  and  $q_{js}$  refer to the  $s$ th element (pixel intensity value) in the  $i$ th principal component vector or the  $j$ th principal component vector.

Then for a given object image (similar but not belonging to the images in the dictionary), each weighting coefficient can be obtained by the inner product between the vector representing the object

image and the vector representing the principal component, shown in Eqs. (4).

$$w_k = \sum_{s=1}^N a_s q_{ks} \quad (4)$$

where  $a_s$  and  $q_{ks}$  refer to the  $s$ th pixel intensity value in the vector representing object image or the  $k$ th principal component vector. This formula exactly matches with the single-pixel imaging model. If  $q_k$  is employed as the illumination pattern, the weighting coefficient  $w_k$  value can be recorded by the single-pixel detector. It shall be noticed that both the object image and illumination patterns are in two-dimensional forms rather than one-dimensional vector in a real SPI system and the 1D/2D conversion is a straightforward re-indexing. In our proposed scheme, first the basis pattern (principal component) matrix  $Q$  is calculated from the object image dictionary containing  $M$  training images by principal component analysis. Then  $K$  most significant principal components are employed as the illumination patterns for single-pixel imaging. For one target object image that does not belong to the image dictionary but has similar image features to the training images, the weighting coefficients can be acquired by the single-pixel detector under the illumination of these principal component patterns. Finally, the target object image can be computationally reconstructed from the acquired single-pixel intensity values (weighting coefficients) and the corresponding illumination patterns, indicated by Eqs. (2).

The pixel intensity values in the principal components and weighting coefficients can be both positive and negative. However, illumination patterns only allow positive element values in a practical optical system. This problem can be easily solved by adding a same DC off-set to each non-negative illumination pattern, shown in Eqs. (5). The DC offset pattern is added as an additional illumination pattern.

$$w_k = \sum_{s=1}^N a_s (DC + q_{ks}) - \sum_{s=1}^N a_s DC \quad (5)$$

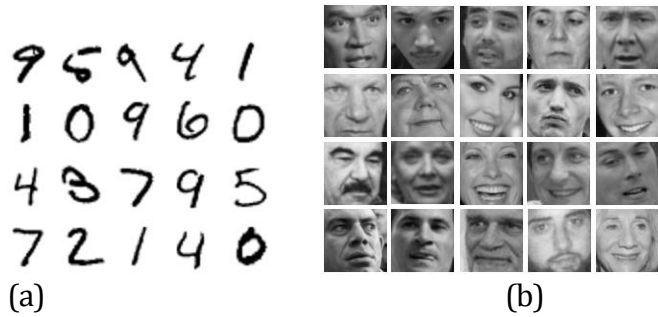
### 3. RESULTS AND DISCUSSION

In our simulation, three different categories of object images, including number digit images from MNIST dataset [43], facial images from LFWcrop dataset [44] and airplane images from CIFAR-10 dataset [45] are assumed to be the original object images in a

single-pixel imaging system. Some examples of images belonging to each category are shown in Fig. 2. Three different sets of illumination patterns are designed for each category of object images correspondingly by extracting the principal components with our proposed scheme described in Section 2. The first ten principal illumination patterns designed with our proposed scheme are shown in Fig. 3 as examples. Then the quality of reconstructed results for each category of testing images under varying number of illuminations in single-pixel imaging is evaluated. The number of training images and testing images taken from each category is three different simulations is presented in Table 1.

**Table 1 Number of training and testing images for each object image category in the simulation**

Category	Image size	Number of training images	Number of testing images
Hand-written digit images	$56 \times 56$	3000	300
Face images	$64 \times 64$	5500	300
Airplane images	$64 \times 64$	4500	300



(c)

Fig. 2. Some image examples in each category of training and testing images: (a) Number digit images from MNIST dataset [43]; (b) Facial images from LFWcrop dataset [44]; (c) Airplane images from CIFAR-10 dataset [45].

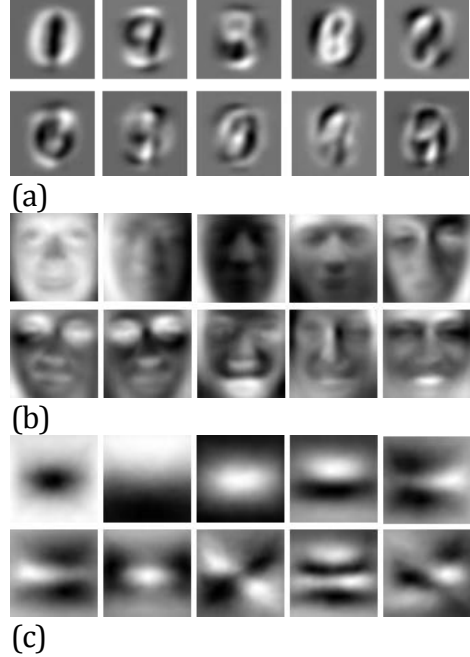


Fig. 3. First ten principal illumination patterns designed in our scheme for (a) number digit images; (b) facial images; (c) airplane images.

The image quality of reconstructed results with illumination patterns designed by our scheme for three categories of testing images is presented in Fig. 3. The image quality is compared with the reconstructed results by conventional Fourier single-pixel imaging (FSPI) [31]. It can be observed that the reconstructed results in our scheme have several dB higher PSNR values than the ones in conventional FSPI for all the three categories of images. The results indicate our proposed scheme can yield better imaging efficiency than conventional FSPI. Among the three categories, the

quality differences for number digit images and facial images are more significant than the difference for airplane images. Some reconstructed images examples are demonstrated in Fig. 5.

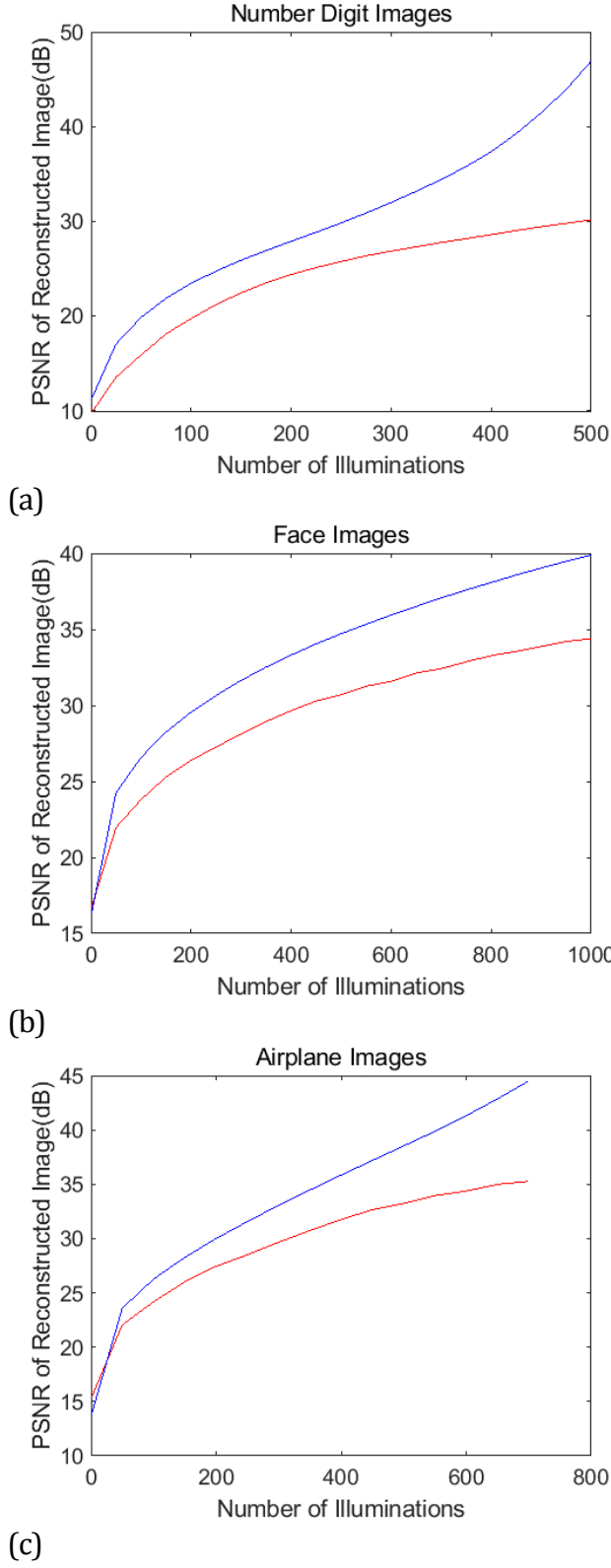
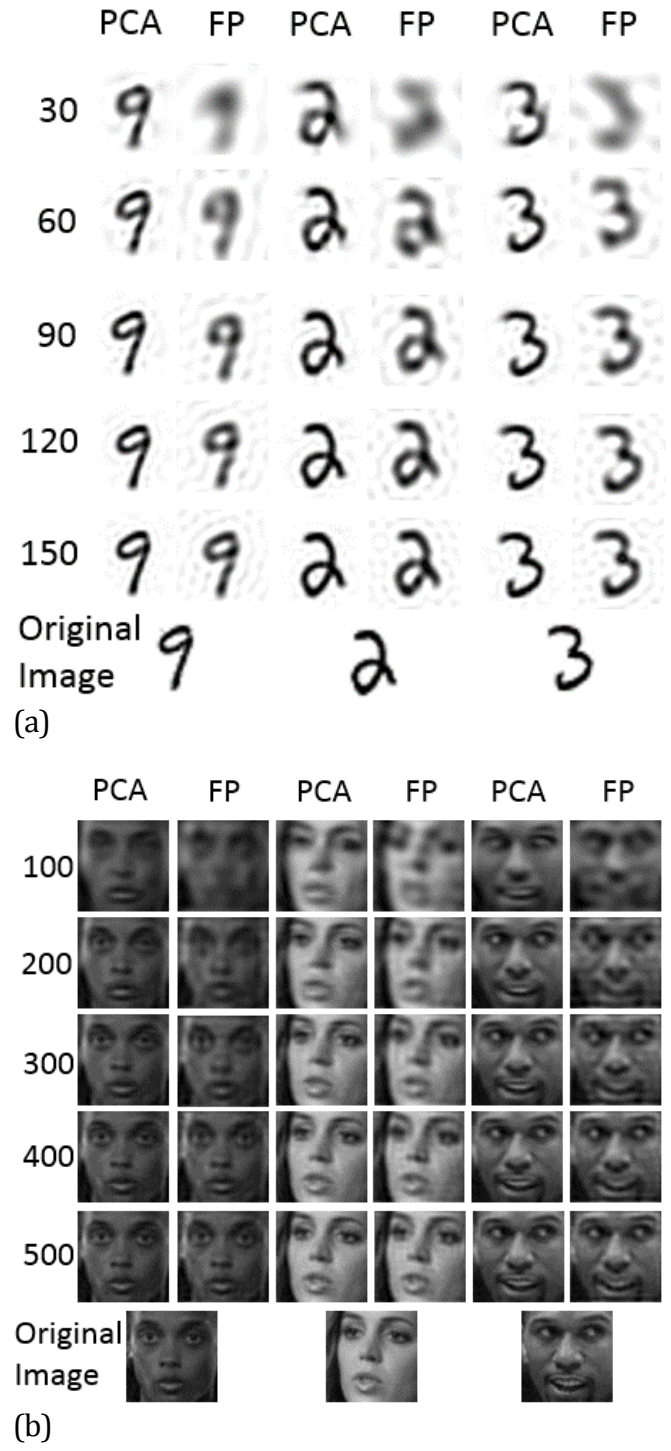


Fig. 4. Image quality (PSNR) of reconstructed results in single-pixel imaging with the illumination patterns designed in our scheme (blue) and conventional Fourier single-pixel imaging (red) for the testing images (a)number digit images; (b)facial images; (c)airplane images.



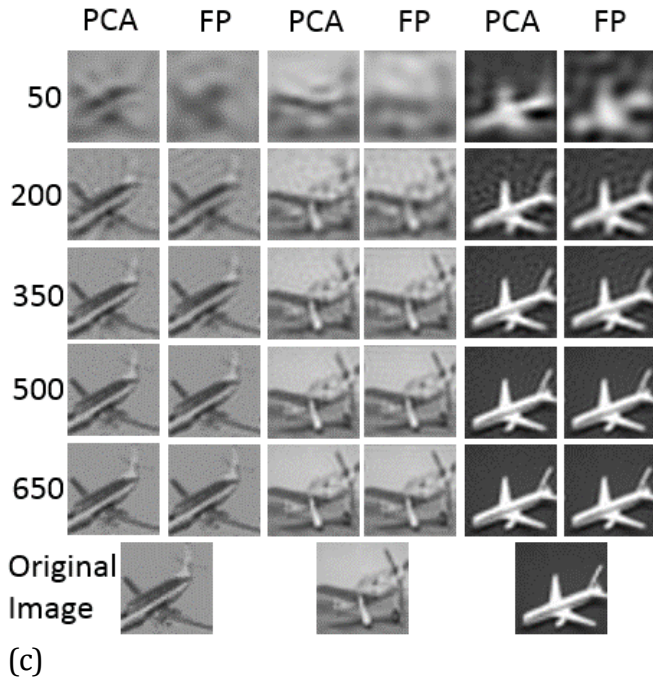


Fig. 5. Three pairs of reconstructed test image examples for each category of images in single-pixel imaging with the illumination patterns designed in our scheme (PCA) and conventional Fourier pattern single-pixel imaging (FP) for varying number of illuminations (each row): (a) number digit images; (b) facial images; (c) airplane images.

The results in Fig. 5 visually reveal the fact that the visual quality of reconstructed object images in our proposed scheme is superior to the ones in Fourier single-pixel imaging. The outperformances of our proposed scheme are more evident for number digit images and facial images, compared to airplane images. It will be more favorable for our proposed scheme if there are more evident similarities and more common features among the images in the given category. The number digit images and facial images in Fig. 2(a) and Fig. 2(b) have many common image features, which can be extracted as principal components (illumination patterns) in Fig. 3(a) and Fig. 3(b). On the other hand, there is less similarity among the images in the airplane dataset (Fig. 2(c)) even though they all semantically belong to “airplanes”. It can be observed that there is not much common feature information extracted in the principal components in Fig. 3(c) from the diversified airplane images. The performance of our proposed scheme depends on how similar between each other the target images are in the specific imaging scenario.

#### 4. CONCLUSION

In single-pixel imaging (SPI), it usually requires a large number of illuminations to obtain high-quality reconstructed object images. The illumination patterns can be appropriately designed in a SPI system to achieve high imaging efficiency. The transform-basis illumination patterns such as Fourier sinusoidal patterns are proposed in previous works and can significantly enhance the imaging efficiency. However, such patterns are fixed and non-adaptive for different categories of object images. The illumination patterns can be adaptively designed and optimized when the SPI system is used in a pre-known specific imaging scenario for a specific type of images. In this work, we propose to collect a certain number of exemplar training images (an image dictionary) for a target object image category and then extract the principal components as the optimal illuminations patterns using the principal component analysis technique. With the illumination patterns designed by our proposed scheme, the reconstructed images in single-pixel imaging have better quality than conventional FSPI under the same number of illuminations. Our proposed scheme can significantly enhance the imaging efficiency in a single-pixel imaging system especially when there are strong similarities and common features among all the possible object images in the imaging scenario.

**Funding Information.** None.

#### References

1. A. Gatti, E. Brambilla, M. Bache, and L. A. Lugiato, “Ghost imaging with thermal light: comparing entanglement and classical correlation,” *Phys. Rev. Lett.* 93, 093602 (2004).
2. J. H. Shapiro, “Computational ghost imaging,” *Phys. Rev. A* 78, 061802 (2008).
3. M. F. Duarte, M. A. Davenport, D. Takhar, J. N. Laska, T. Sun, K. F. Kelly, and R. G. Baraniuk, “Single-pixel imaging via compressive sampling,” *IEEE Signal Proc. Mag.* 25, 83-91 (2008).
4. W. Chan, K. Charan, D. Takhar, K. Kelly, R. Baraniuk, and D. Mittleman, “A single-pixel terahertz imaging system based on compressed sensing,” *Appl. Phys. Lett.* 93, 121105 (2008).
5. B. I. Erkmen, “Computational ghost imaging for remote sensing,” *J. Opt. Soc. Am. A* 29, 782–789 (2012).
6. B. Sun, M. P. Edgar, R. Bowman, L. E. Vittert, S. Welsh, A. Bowman and M. J. Padgett, “3-D Computational imaging with single-pixel detectors,” *Science* 340, 844-847 (2013).
7. M.-J. Sun, M. P. Edgar, G. M. Gibson, B. Sun, N. Radwell, R. Lamb and M. J. Padgett, “Single-pixel three-dimensional imaging with timebased depth resolution,” *Nat. Commun.* 7, 12010 (2016).
8. Z. Zhang, S. Liu, J. Peng, M. Yao, G. Zheng, and J. Zhong, “Simultaneous spatial, spectral, and 3D compressive imaging via efficient Fourier single-pixel measurements,” *Optica* 5, 315-319 (2018).

9. N. Radwell, K. J. Mitchell, G. M. Gibson, M. P. Edgar, R. Bowman and M. J. Padgett, "Single-pixel infrared and visible microscope," *Optica* 1, 285-289 (2014).
10. R. S. Aspden, N. R. Gemmell, P. A. Morris, D. S. Tasca, L. Mertens, M. G. Tanner, R. A. Kirkwood, A. Ruggeri, A. Tosi, R. W. Boyd, G. S. Buller, R. H. Hadfield and M. J. Padgett, "Photon-sparse microscopy: visible light imaging using infrared illumination," *Optica* 2, 1049 (2015).
11. E. Tajahuerce, V. Durán, P. Clemente, E. Irles, F. Soldevila, P. Andrés and J. Lancis, "Image transmission through dynamic scattering media by single-pixel photodetection," *Opt. Express* 22, 16945-16955 (2014).
12. L. Bian, J. Suo, G. Situ, Z. Li, J. Fan, F. Chen and Q. Dai, "Multispectral imaging using a single bucket detector," *Sci. Rep.* 6, 24752 (2016).
13. D. Pelliccia, A. Rack, M. Scheel, V. Cantelli and D. M. Paganin, "Experimental x-ray ghost imaging," *Phys. Rev. Lett.* 117, 113902 (2016).
14. P. Clemente, V. Durán, E. Tajahuerce and J. Lancis, "Optical encryption based on computational ghost imaging," *Opt. Lett.* 35, 2391-2393 (2010).
15. W. Chen and X. Chen, "Object authentication in computational ghost imaging with the realizations less than 5% of Nyquist limit," *Opt. Lett.* 38, 546-548 (2013).
16. C. Zhao, W. Gong, M. Chen, E. Li, H. Wang, W. Xu and S. Han, "Ghost imaging lidar via sparsity constraints," *Appl. Phys. Lett.* 101, 141123 (2012).
17. W. Gong, C. Zhao, H. Yu, M. Chen, W. Xu and S. Han, "Three-dimensional ghost imaging lidar via sparsity constraint," *Sci. Rep.* 6, 26133 (2016).
18. G. M. Gibson, B. Sun, M. P. Edgar, D. B. Phillips, N. Hempler, G. T. Maker, G. P. Malcolm and M. J. Padgett, "Real-time imaging of methane gas leaks using a single-pixel camera," *Opt. Express* 25, 2998-3005 (2017).
19. F. Ferri, D. Magatti, L. A. Lugiato, and A. Gatti, "Differential ghost imaging," *Phys. Rev. Lett.* 104, 253603 (2010).
20. B. Sun, S. S. Welsh, M. P. Edgar, J. H. Shapiro, and M. J. Padgett, "Normalized ghost imaging," *Opt. Express* 20, 16892-16901 (2012).
21. O. Katz, Y. Bromberg, and Y. Silberberg, "Compressive ghost imaging," *Appl. Phys. Lett.* 95, 131110 (2009).
22. L. Bian, J. Suo, Q. Dai, and F. Chen, "Experimental comparison of single-pixel imaging algorithms," *J. Opt. Soc. Am. A*, 35, 78-87 (2018).
23. W. Wang, X. Hu, J. Liu, S. Zhang, J. Suo, and G. Situ, "Gerchberg-Saxton-like ghost imaging," *Opt. Express* 23, 28416-28422 (2015).
24. X. Hu, J. Suo, T. Yue, L. Bian, and Q. Dai, "Patch-primitive driven compressive ghost imaging," *Opt. Express* 23, 11092-11104 (2015).
25. C. Zhang, S. Guo, J. Cao, J. Guan, and F. Gao, "Object reconstitution using pseudo-inverse for ghost imaging," *Opt. Express* 22, 30063-30073 (2014).
26. X. Zhang, X. Meng, X. Yang, Y. Wang, Y. Yin, X. Li, X. Peng, W. He, G. Dong, and H. Chen, "Singular value decomposition ghost imaging," *Opt. Express* 26, 12948-12958 (2018).
27. M. Lyu, W. Wang, H. Wang, H. Wang, G. Li, N. Chen and G. Situ, "Deep-learning-based ghost imaging," *Sci. Rep.* 7, 17865 (2017).
28. T. Shimobaba, Y. Endo, T. Nishitsui, T. Takahashi, Y. Nagahama, S. Hasegawa, M. Sano, R. Hirayama, T. Kakue, A. Shiraki and T. Ito, "Computational ghost imaging using deep learning," *Opt. Commun.* 413, 147-151 (2018).
29. C. F. Higham, R. Murray-Smith, M. J. Padgett and M. P. Edgar, "Deep learning for real-time single-pixel video," *Sci. Rep.* 8, 2369 (2018).
30. Y. He, G. Wang, G. Dong, S. Zhu, H. Chen, A. Zhang and Z. Xu, "Ghost Imaging Based on Deep Learning," *Sci. Rep.* 8, 6469 (2018).
31. Z. Zhang, X. Ma, and J. Zhong, "Single-pixel imaging by means of Fourier spectrum acquisition," *Nat. Commun.* 6, 6225 (2015).
32. L. Wang, and S. Zhao, "Fast reconstructed and high-quality ghost imaging with fast Walsh-Hadamard transform," *Photonics Res.* 4, 240-244 (2016).
33. B. L. Liu, Z. H. Yang, X. Liu, and L. A. Wu, "Coloured computational imaging with single-pixel detectors based on a 2D discrete cosine transform," *J. Mod. Optic.* 64, 259-264 (2017).
34. M. Alemohammad, J. R. Stroud, B. T. Bosworth, and M. A. Foster, "High-speed all-optical Haar wavelet transform for real-time image compression," *Opt. Express* 25, 9802-9811 (2017).
35. M. Li, R. He, Q. Chen, G. Gu, and W. Zhang, "Research on ghost imaging method based on wavelet transform," *J. Opt.* 19(9), 095202 (2017).
36. W. K. Yu, M. F. Li, X. R. Yao, X. F. Liu, L. A. Wu, and G. J. Zhai, "Adaptive compressive ghost imaging based on wavelet trees and sparse representation," *Opt. Express.* 22, 7133-7144 (2014).
37. H. Abdi, and L. J. Williams, "Principal component analysis," *WIREs. Comput. Stat.* 2, 433-459 (2010).
38. S. Jiao, Z. Zhuang, and W. Zou, "Fast computer generated hologram calculation with a mini look-up table incorporated with radial symmetric interpolation," *Opt. Express* 25, 112-123 (2017).
39. C. Zuo, Q. Chen, W. Qu, and A. Asundi, "Phase aberration compensation in digital holographic microscopy based on principal component analysis," *Opt. Lett.* 38, 1724-1726 (2013).
40. S. Yeom, B. Javidi, P. Ferraro, D. Alfieri, S. DeNicola, and A. Finizio, "Three-dimensional color object visualization and recognition using multi-wavelength computational holography," *Opt. Express* 15, 9394-9402 (2007).
41. Q. Du, and J. E. Fowler, "Hyperspectral image compression using JPEG2000 and principal component analysis," *IEEE Geosci. Remote S.* 4, 201-205 (2007).
42. H. Gao, J. F. Cai, Z. Shen, and H. Zhao, "Robust principal component analysis-based four-dimensional computed tomography," *Phys. Med. Biol.* 56, 3181 (2011).
43. L. Deng, "The MNIST database of handwritten digit images for machine learning research," *IEEE Signal Proc. Mag.* 29, 141 (2012).
44. G.B. Huang, M. Ramesh, T. Berg, and E. Learned-Miller, "Labeled Faces in the Wild: A Database for Studying Face Recognition in Unconstrained Environments," University of Massachusetts, Amherst, Technical Report 07-49, 2007.
45. Alex Krizhevsky, "Learning Multiple Layers of Features from Tiny Images," 2009.